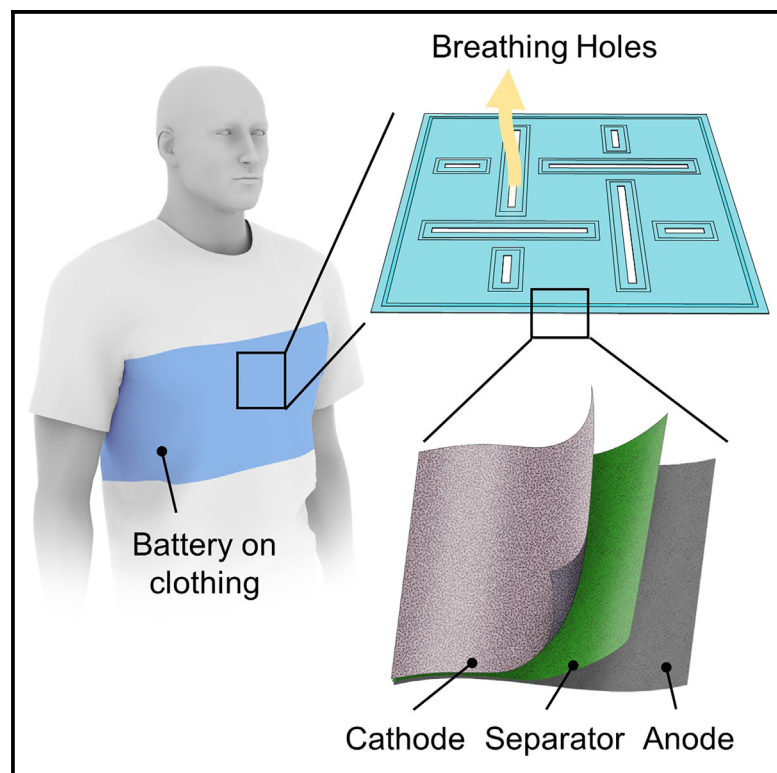


Stretchable, breathable, wearable batteries using a holey design

Graphical abstract



Highlights

- The holey battery achieves high breathability while preserving high energy density
- It demonstrates stable electrochemical performance under stretching and folding
- It is compatible with conventional battery fabrication techniques

Authors

Lin Xu, Qiongyu Chen,
Sumedha Vishalini Pichchamuttu, ...,
Ping Liu, Teng Li, Liangbing Hu

Correspondence

lit@umd.edu (T.L.),
liangbing.hu@yale.edu (L.H.)

In brief

A novel “holey” battery architecture with carefully placed holes creates stretchable, breathable, and comfortable energy storage for wearable devices. This design maintains high capacity and stability even under bending and stretching, and it can be produced by standard manufacturing methods. Twice as breathable as cotton, it ensures user comfort, expanding the potential of seamlessly integrating battery technology into everyday clothing and accelerating the practical adoption of wearable electronics.



Development

Practical, real world, technological considerations and constraints

Xu et al., 2025, Matter 8, 101959
March 5, 2025 © 2025 Elsevier Inc. All rights are reserved, including those for text and data mining, AI training, and similar technologies.
<https://doi.org/10.1016/j.matt.2025.101959>

Article

Stretchable, breathable, wearable batteries using a holey design

Lin Xu,^{1,2,12} Qiongyu Chen,^{3,12} Sumedha Vishalini Pichchamuttu,^{1,4,12} Lianping Wu,³ Elijah Pate,⁵ Christine Wu,⁶ Tangyuan Li,^{1,2} Xueying Zheng,¹ Chong Yang,^{1,2} Kexia Jin,¹ Ping Liu,^{7,8,9} Teng Li,^{3,*} and Liangbing Hu^{1,2,10,11,13,*}

¹Department of Materials Science and Engineering, University of Maryland, College Park, MD 20742, USA

²Department of Electrical and Computer Engineering, Yale University, New Haven, CT 06511, USA

³Department of Mechanical Engineering, University of Maryland, College Park, MD 20742, USA

⁴Institute for Physical Science and Technology (IPST), University of Maryland, College Park, MD 20742, USA

⁵Mount Saint Joseph High School, 4403 Frederick Avenue, Baltimore, MD 21229, USA

⁶The Lawrenceville School, 2500 Main Street, Lawrenceville, NJ 08648, USA

⁷Program of Materials Science, University of California, San Diego, La Jolla, CA 92093, USA

⁸NanoEngineering Department, University of California, San Diego, La Jolla, CA 92093, USA

⁹Program of Chemical Engineering, University of California, San Diego, La Jolla, CA 92093, USA

¹⁰Center for Materials Innovation, Yale University, New Haven, CT 06511, USA

¹¹Department of Materials Science, Yale University, New Haven, CT 06511, USA

¹²These authors contributed equally

¹³Lead contact

*Correspondence: lit@umd.edu (T.L.), liangbing.hu@yale.edu (L.H.)

<https://doi.org/10.1016/j.matt.2025.101959>

PROGRESS AND POTENTIAL The development of the holey battery design marks significant progress toward fully wearable energy storage devices that maintain high performance under deformation and sustain wearer comfort. By integrating finite element method (FEM)-guided hole patterns, the new architecture achieves notable improvements in stretchability, flexibility, and breathability without compromising areal energy density. Remarkably, the holey structure preserves electrochemical performance even under deformations, as demonstrated by stable capacity retention over multiple cycles and recoverable capacity after 10% diagonal stretching or 180° folding. Moreover, the straightforward fabrication process—relying on conventional electrode materials, consumables, and hot pressing—lowers the manufacturing complexity and is readily scalable. The breathability, measured to be twice that of cotton cloth, ensures that the battery's integration into clothing will not diminish comfort, opening pathways toward next-generation wearable electronics that are both practical and user friendly. As such, this holey battery concept not only evidences impressive current achievements but also highlights a promising potential for large-scale, cost-effective production and broad application in wearable technologies.

SUMMARY

The rigid and non-breathable nature of conventional batteries has remained a significant limitation on wearable electronics, particularly in applications involving dynamic physical activities. Herein, we present a "holey" battery design, which is both breathable and deformable while maintaining high energy density and ease of fabrication. Guided by the finite element method (FEM), this design incorporates a strategic array of holes within a standard pouch cell framework that significantly enhances the battery's breathability (twice as much as conventional cotton) and stretchability—maintaining robust electrochemical performance under 10% stretching deformation. Importantly, this architecture allows for a high areal energy density, achieving 7.2 mW h/cm² in a single-layer pouch, which is scalable to 14.4 mW h/cm² using double electrode layers. The battery is resilient under physical stress, including 10% diagonal stretching (>90% capacity) and 180° folding (>95% capacity), with quick recovery upon release, marking a significant advance in the field of e-textiles.

INTRODUCTION

Flexible electronics has revolutionized the textile industry, ushering in an era where textiles are not just for comfort and style but also enhance our daily lives and well-being.^{1–9} However, a crucial aspect that has hindered the full potential of wearable devices is the rigid nature of current commercially available batteries, which can limit the flexibility and usability of the devices.^{10–17} Furthermore, during athletic or physical activities, garments are subjected to dynamic stretching movements. The inherent rigidity of conventional battery systems poses a significant constraint on such movements. For example, during running, the chest width may experience an expansion of approximately 10%,¹⁸ underscoring the necessity for batteries to exhibit enough stretchability to align with the demands of wearable applications. Such flexibility is imperative not only for wearer comfort but also for the functional integrity of the garment, ensuring seamless integration with the body's natural movements. Additionally, a significant challenge arises from the necessity to fully seal batteries to ensure their functionality, leading to poor breathability.^{19–22} This lack of breathability is a substantial drawback for wearable electronics and textiles, as it can cause discomfort by trapping heat and moisture against the skin, leading to excessive sweating and an overall uncomfortable experience for the user. Consequently, the development of batteries that are not only flexible and stretchable but also breathable is of paramount importance.^{23–25} Additionally, for the purpose of cost reduction, the ease of fabrication must be a key consideration in the design and production of wearable batteries.

Extensive research has been undertaken to address these challenges in wearable battery technology. Initial studies have focused on the use of flexible substrates in battery construction.^{26–32} For example, the work of Meng et al. utilized a Cu-deposited conductive nonwoven cloth as the substrate material with a wave-like device architecture to achieve electrode flexibility sufficient for use on curved surfaces, like watch straps.³³ Additionally, Pu et al. demonstrated a flexible lithium-ion battery (LIB) belt using Ni-cloth textile as a substrate and an Al pouch as the package.² The LIB belt exhibited decent electrochemical performance even when bent, ensuring the feasibility of wearing it as a waist belt, etc. However, these materials, while flexible, are not inherently stretchable, limiting their use in scenarios involving significant strain, such as active sports. To address this, researchers have explored using elastic materials for both substrates and battery packaging.^{34–39} For example, Kumar et al. utilized poly-styrene-block-polyisoprene-block-polystyrene (SIS) as a hyper-elastic binder, enabling the battery to accommodate the substantial elastic strain experienced during vigorous activities.³⁴ Despite this improvement in stretchability, the use of elastic substrates often necessitates inactive additives in the electrode materials to maintain performance under stretching, which reduces the overall energy density of the battery.³⁶ Moreover, both flexible and elastic battery designs require effective sealing, which compromises the breathability.

A promising solution has been the development of fiber-shaped batteries.^{6,7,23,24,40–46} This innovative design typically involves using conductive wires (e.g., metal) as substrates for

electrode materials, intertwining anode and cathode wires, and sealing them with polymer packaging.²⁴ Since these batteries mimic the geometry of yarns, they can be directly woven or knitted into clothing, offering similar deformability and breathability. However, this design is not without its drawbacks. The fabrication complexity of fiber-shaped batteries is considerable, requiring unique manufacturing procedures and equipment, complicating large-scale commercialization and hindering straightforward adoption in the market.⁶ Furthermore, while these fiber-shaped batteries are bendable and twistable, their stretchability is limited due to the rigidity of the metal core, posing a challenge for certain applications.⁴¹

Herein, we demonstrate a breathable and stretchable battery design enabled by the strategic placement of rectangular holes that extend through a conventional pouch cell (Figure 1A). Prior research has explored various bendable and foldable structures in flexible electronics by implementing open-hole designs.^{47–49} For instance, Rogers et al. describe electronic devices that leverage non-traditional geometries or structures of semiconductors to impart desirable mechanical properties, such as flexibility and stretchability.^{50,51} In our approach, we extend this concept to battery systems, demonstrating its efficacy in enhancing structural deformability. The hole pattern is determined via the finite element method (FEM) to reduce the strain under different deformation states while keeping a small hole area for optimal areal energy density. The periphery of each hole is sealed to ensure no leakage, while the design otherwise maintains the foundational architecture of conventional pouch cells, including a cathode foil, anode foil, separator infused with electrolyte, and laminated aluminum packaging for passivation. The inclusion of holes in the battery's structure promotes air circulation, effectively mitigating heat accumulation and moisture retention. Notably, the breathability of this holey cell design surpasses that of cotton cloth. Moreover, the holes significantly enhance the battery's stretchability compared to pristine pouch cells without holes. For example, we subject the holey battery to a 10% stretching deformation and observed little impact on its performance. Additionally, this design does not impose extra requirements on the cathode and anode materials, allowing the use of commercially available electrodes with no additional non-active material. Consequently, the areal energy density of the cell is preserved at a high level of 7.2 mWh/cm² for a single-layer holey battery pouch, which can be further increased by incorporating multiple electrode layers. Typical wearable devices operate with a power consumption at the mW level.^{52–54} Using our holey battery as an example, a capacity of 7.2 mWh/cm² would allow a mW-level sensor to operate for ~7.2 h per cm² of battery area. Thus, a 4 cm² battery could sustain a device for a full day.

A comparative analysis with prior studies on the stretchability, breathability, and areal energy density of wearable batteries is presented in Figure 1B, and the results are summarized in Table S1. We also calculated and compared the gravimetric energy density and volumetric energy density with other wearable batteries studies, as shown in Table S2. Additionally, it is one of the few designs, apart from fiber-shaped batteries, to offer significant breathability. However, this holey battery design stands out for its high areal energy density and excellent

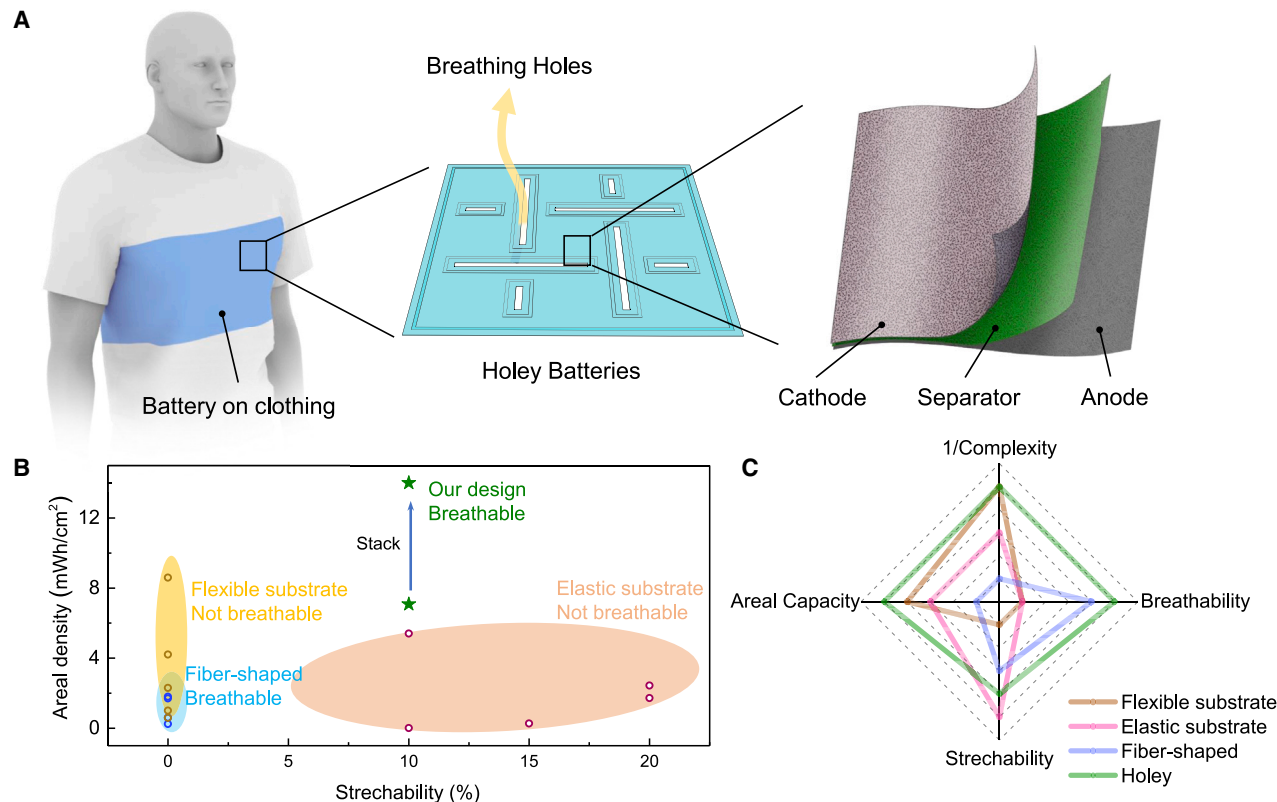


Figure 1. Schematic of holey batteries

(A) Schematic of the holey battery design for wearable applications. Holes were designed throughout the battery pouch to achieve greater breathability and stretchability for improved comfort and wear. Conventional battery materials (cathode, anode, electrolyte/separator) are placed between packaging materials, excluding the hole areas. This design allows for the attachment of the holey battery onto clothing via weaving for use in wearable electronics applications.

(B) Comparison of the areal density and stretchability between our holey battery design and other reports of wearable batteries (see [Table S1](#)).^{19–21,27–29,33,35–37,40–42,48}

(C) Qualitative performance evaluation of the holey battery design in comparison with other wearable battery research studies (see [Table S3](#) for more details).

stretchability compared to fiber-based batteries. It is also relatively simple to fabricate compared to alternatives like elastic substrates, which require varied passivation materials, and fiber-shaped batteries, which employ an entirely different fabrication system, as illustrated in [Figure 1C](#). This holey battery design presents a promising and scalable method for fabricating comfortable, wearable batteries for wearable electronics.

RESULTS AND DISCUSSION

To determine the configuration for the battery holes, we used the FEM to evaluate the distribution of strain under different deformation conditions and different hole shapes. All modeled battery pouches have a side length of 10 cm, while the areas of the holes are kept the same for holes with different shapes and patterns. We first studied how strain was concentrated on battery pouches that featured a single centered hole in the shape of a circle, square, or cross while applying a 3% horizontal edge stretch. The distribution of the maximum principal strain after stretching is shown in [Figure S1](#). While stretching, the battery pouch with a single circular hole exhibited significant strain local-

ized near the two edges of the circular hole perpendicular to the stretch direction. Over 2/3 of the pouch area adjacent to the two circle edges show strains greater than the applied stretch. Moreover, the strain level of the most concentrated area is ~9%, approximately three times the applied stretch, per the well-known analytical solution from Timoshenko.⁵⁵ Similar strain levels and distribution are also present in the pouch with a single square hole. The strain localizations near the holes are evident; since the overall elongation of the battery pouch is accommodated mainly by a pure in-plane stretch,⁵⁶ minor deflection toward the out-of-plane direction can be observed from the two simulated cases. In contrast, although the strain level of the localized area near the tip of the cross hole is higher than 9% due to a smaller circle radius, the region with a strain level higher than the applied stretch is significantly reduced to 1/3 of the total area of the pouch. The region adjacent to the single cross hole remains at a low strain level. Such strain deconcentration benefits from bulging the cross hole toward the out-of-plane direction.

Inspired by this strain mitigation mechanism, we extended the edge stretch simulation to battery pouches with arrayed holes in

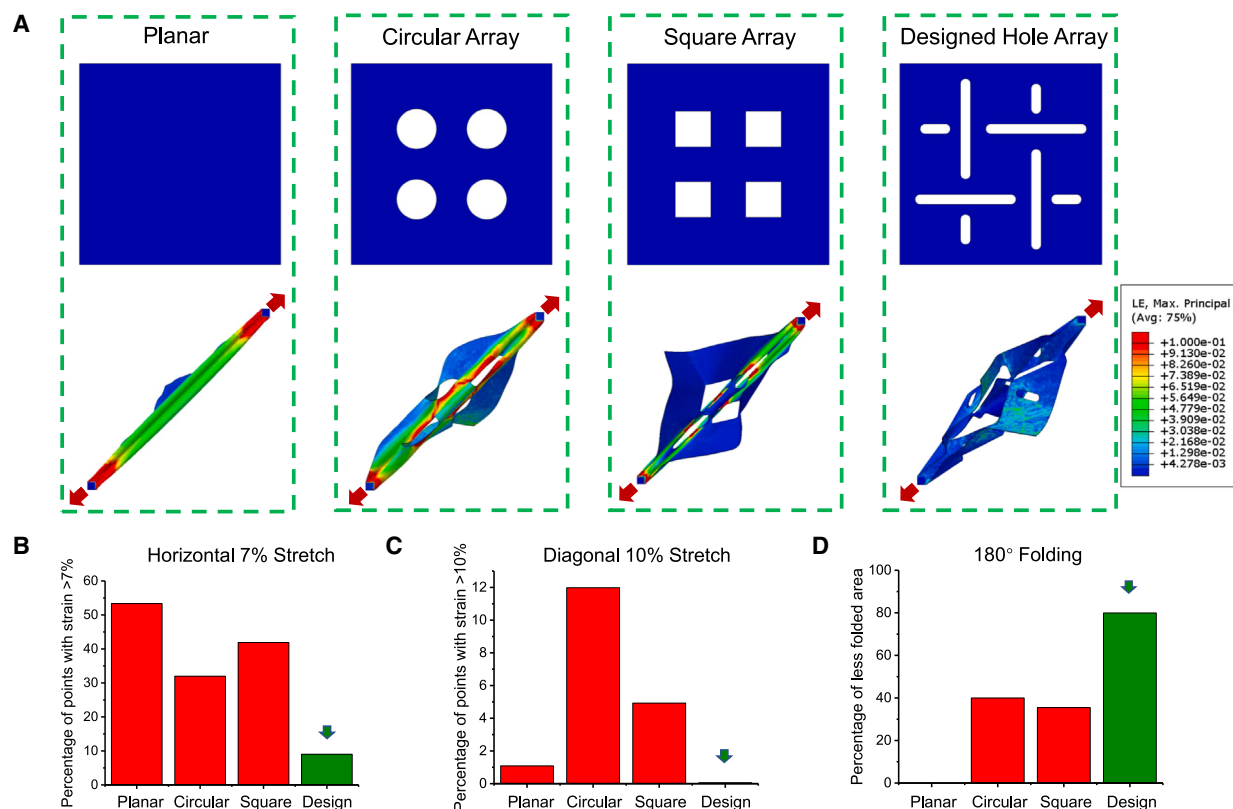


Figure 2. FEA of batteries with different hole patterns

(A) Strain distribution in four designs of battery pouches: with no breathing holes (planar), with circular arrayed breathing holes, with square arrayed breathing holes, and with the designed hole array before (top row) and after (bottom row) 10% diagonal elongation. The contour color plots the maximum principal strain in the battery pouch.

(B) Percentage of area with maximum principal strain greater than 7% in the four types of battery pouches under 7% edge stretch.

(C) Percentage of area with maximum principal strain greater than 10% in the four types of battery pouches under 10% diagonal stretch.

(D) Percentage of the less folded area of the four types of battery pouches under folding.

various shapes and compared them with the one with no holes, as shown in Figure S2. Under a 7% horizontal edge stretch, the planar battery pouch exhibits strain of no less than 7% across the regions, indicating the absence of a strain deconcentration effect. In the case of pouches with circular and square arrayed holes, while the strains in several regions near the arrayed holes are lower than the applied stretch, the majority of the pouches are still in significantly high in-plane tension, as evidenced by the wrinkling patterns appearing at the pouch center. On the other hand, the battery pouch with our designed hole array shows an impressive strain deconcentration effect due to its superior out-of-plane deformability. In Figure S2, we see the out-of-plane deflections in all directions, enabled by our designed hole array, which reduced the strain to 1% or less in the central region.

We further studied the strain deconcentration effect of the battery pouch with our designed hole array when stretched in the diagonal direction, along with the other 3 cases, as shown in Figure 2A. When stretched by 10% in the diagonal direction, all the other 3 cases start to exhibit tensile instability to accommodate such large stretching, with the planar battery pouch twisting

and the circular and square arrayed hole battery pouches undergoing complex bending. Both deformation modes help them deconcentrate the strain caused by large tension. Nevertheless, the strain levels of the regions along the stretch line are still higher than the applied stretch, which will ultimately impair the deformability of the battery. In contrast, the battery pouch with our designed hole array shows excellent stretchability and a pronounced strain deconcentration effect under diagonal stretch, with a strain of less than 2% in most regions of the material—a five-times reduction compared to the applied stretch. Due to our designed hole array, the battery pouch is free to deflect in all directions to simultaneously accommodate large stretching and optimize the strain deconcentration effect, thus substantially improving its stretchability in all directions.

We also calculated the percentage of the area (number of elements in the model) with strain higher than the applied stretch and thus quantitatively measured the strain concentration effect in the four types of battery pouches. In the case of horizontal edge stretch (Figure 2B), we find that only 9% of the regions in the battery with our designed breathing hole array possess strain higher than the 7% applied edge stretch, which is significantly

lower than those of the planar battery (53.35%), the battery with circular arrayed holes (31.98%), and the battery with the square arrayed holes (41.88%). In the case of the diagonal stretch (Figure 2C), almost none of the regions (0.06%) in the battery with our designed breathing hole array possesses strain higher than the applied 10% diagonal stretch, indicating its outstanding stretchability along its diagonal direction. We also investigated the flexibility of our designed hole battery, along with the other 3 cases, in other extremely large deformation cases, such as folding. To simulate the folding, we set the bending radius as small as 0.5 mm (twice the thickness of the battery pouch). All four types of battery pouches, with or without breathing holes, present exceptional foldability with strains as low as 0.2% and 7% along the folding line when folded by 90° (Figure S3) and 180° (Figure S4), respectively. We attribute such exceptional foldability to the ultralow bending stiffness of the battery due to the pouch's low thickness. Nevertheless, considering the needs of long-time usage (e.g., cyclic folding), we still need to reduce the folded areas as much as possible to extend the battery life. To this end, our designed hole array battery remarkably reduced the folded area by 79.95%, compared to the planar battery with no holes, when being folded along the holes, nearly two times the reduced areas by the batteries with circular arrayed (39.98%) and square arrayed breathing holes (35.46%), as illustrated in Figure 2D.

Samples of holey batteries with the designed hole array were fabricated for mechanical and electrochemical testing. The fabrication process of the holey batteries closely mirrors that of conventional pouch cells. In this process, laminated aluminum foils are utilized as the packaging layer, while aluminum foil coated with cathode materials and copper foil with anode materials are interspersed with a separator saturated in electrolyte, as depicted in Figure 3A. The construction of the example holey batteries involved the utilization of LiFePO_4 (LFP), with a mass loading of 15 mg/cm^2 , as the cathode material, and graphite, with a mass loading of 7 mg/cm^2 , serving as the anode. The electrodes, electrolyte, and packaging materials employed do not necessitate any additional requirements, thereby enabling the use of commercially available materials instead of novel chemicals. Holes, as predetermined by the FEM designs, are then cut through all the material and packaging layers using a razor blade. Alternatively, precise hole fabrication for scalable production can be achieved using techniques such as laser cutting or mechanical die cutting.^{57–59} Die cutting was particularly effective for long production runs due to its ability to produce high-quality, uniform holes. In contrast, laser cutting provided a more flexible and faster process for layout adjustments, though it required the careful optimization of process parameters to avoid burning the printed layer or substrate near the hole edges and was best suited as the first step in the fabrication process. Notably, the hole in the packaging layer is 1.5 mm smaller on each side than that in the separator layer, while the holes in the electrode layers are the largest. This configuration allows for the sealing of both packaging layers around the hole area, ensuring that the electrodes remain completely isolated by the separator. A modified hot-pressing technique is employed to seal the hole edges, involving the integration of an additional heating bar into a standard hot presser (Figure S5). The dimensions of this

heating bar correspond precisely to the hole area, facilitating targeted sealing around the hole upon the application of pressure. Following the sealing of all holes with the presser, the outer periphery of the cell is sealed using a conventional vacuum hot sealer. Scanning electron microscopy (SEM) images of the cathode and anode corners before and after cycling show that the edges of the electrode materials remained intact, with no major damage from hot pressing (Figure S6). The electrolyte is introduced prior to this final sealing stage, completing the fabrication process (see methods for details).

We then evaluated the breathability, stretchability, and functionality of the battery to determine its performance for wearable devices. Breathability assessments were conducted using an upright cup test,⁶⁰ as illustrated in Figure S7. In this test, a silica gel desiccator was placed inside a jar with an inner diameter of 3 in. The battery samples were then sealed to the top surface of these jars with double-sided tape, which were then placed in an environmental chamber with a controlled relative humidity of 70% and a temperature of 25°C. The results of the breathability test are summarized in Figure S8. Comparatively, the breathability of the holey battery outperformed that of the conventional cotton cloth. The rate of water absorption with the holey battery was about twice as much as that of cotton cloth. This finding suggests that integrating the holey battery into clothing should not compromise the garment's breathability. In stark contrast, conventional batteries with a continuous pouch exhibit no breathability.

The battery's operational capability to light up light-emitting diode (LED) lightbulbs under conditions of 10% stretching along diagonal and 180° folding was also verified, as demonstrated in Figures 3B and 3C (Videos S1 and S2). The shapes of the batteries under deformation are consistent with the simulated shape predicted by the FEM model (Figure S9). This demonstrates the accuracy of the FEM model. Furthermore, the battery was integrated into a lab coat using cotton yarn, and its functionality was tested under various activities, including running. Figure 3D showcases the ability of the holey battery to power LEDs in both static and dynamic (running) states, thereby further suggesting its suitability for use in wearable devices (Video S3).

As illustrated in Figure 4A, the holey battery, when free of deformation and subjected to a discharge current density of 75 mA/g, demonstrated an initial discharge capacity of 149 mA h/g and excellent cycling stability. Its capacity retention exceeded 95% over the span of 100 cycles (Figure 4E). This finding indicates that the presence of holes within all material layers does not detrimentally impact the battery's electrochemical performance.

The electrochemical performance of holey batteries under various deformation modes was comprehensively assessed, as depicted in Figures 4B–4D. The tests involved subjecting the holey battery to alternating cycles between a free-standing mode and a 10% diagonal stretch mode, each comprising 20 charge-discharge cycles. As shown in Figure 4F, the application of a 10% diagonal stretch to the holey battery did not hinder its discharge capability, maintaining over 90% of its capacity relative to the free-standing mode. This resilience can be attributed to the strategically designed hole pattern, which effectively minimizes the fraction of the battery subjected to significant strain

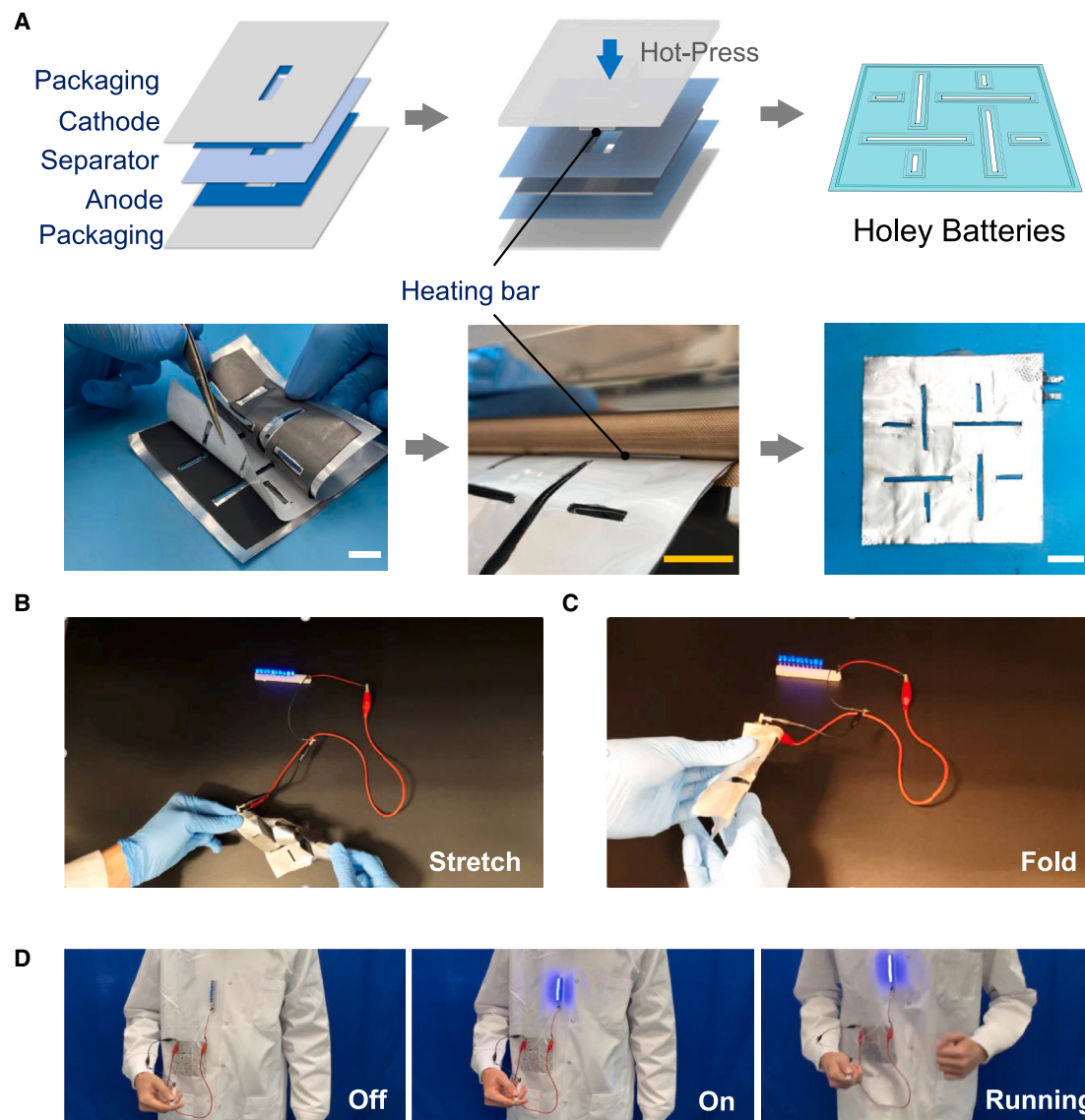


Figure 3. Fabrication and performance of holey batteries

(A) Schematic and digital images illustrating the fabrication process of the holey batteries. Initially, holes with the designated pattern were precisely cut into laminated aluminum foils, electrode foils, and separators using a razor blade. Hot pressing was then employed to seal the hole area, with an additional heating bar integrated into the standard hot presser for precise heating around the hole. The outer periphery of the cell was sealed using a conventional vacuum hot sealer (scale bar: 2 cm).

(B) The battery demonstrates operational functionality at a 10% stretch along the diagonal direction, even after 100 stretch/release cycles.

(C) The battery exhibits operational capability after undergoing 180° folding, even after 100 folding/release cycles.

(D) Upon being woven onto a lab coat, the battery serves as a functional power source for wearable devices and remains operational during dynamic activities such as running or other physical exercises.

that could otherwise cause degradation or failure. Additionally, the battery's cycling stability during the stretch state was noteworthy, with the capacity swiftly recovering upon reverting to the free-standing state and the alleviation of strain. This behavior was consistently observed during the second stretch-release cycle, demonstrating the battery's capability to withstand repetitive stretching movements typical in active sport scenarios. We also evaluated the battery's performance during a 180°

folding-unfolding cycle, as shown in Figure 4G. The incorporation of holes significantly reduced the area subjected to large strain during folding, enabling the maintenance of more than 95% of the battery's capacity during folding, compared to its free-standing state. The capacity also recovered upon the release of the folding force. We also tested the performance of a cell without holes under 180° folding, observing a slight decrease in capacity compared to the cell with holes. This

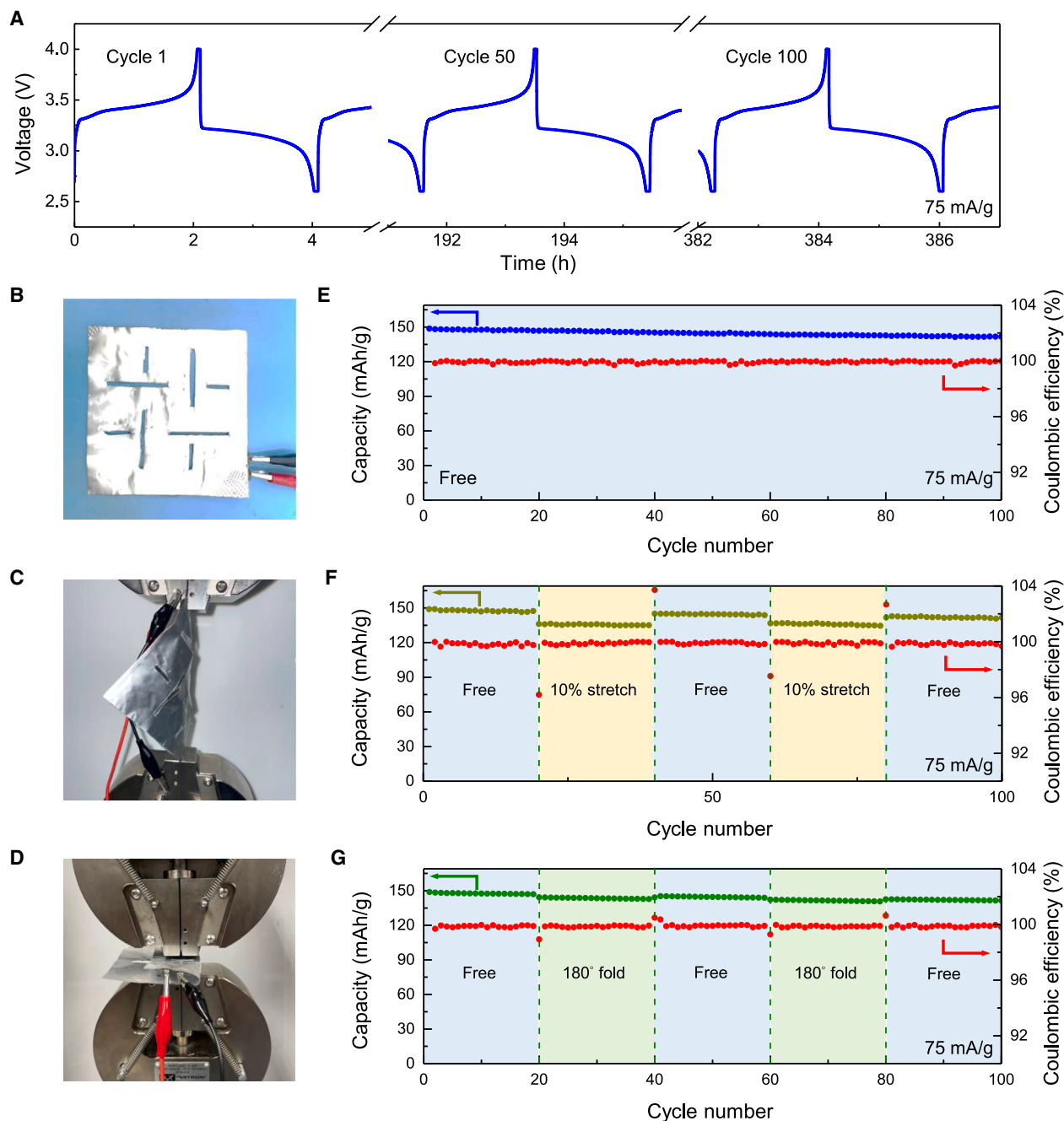


Figure 4. Electrochemical performance of the holey batteries under deformation

(A) Charge-discharge profile of the holey battery without deformation.

(B–D) Images depicting holey batteries during electrochemical tests in their undeformed state (B), when stretched diagonally by 10% (C), and when folded 180° (D).

(E–G) Discharge capacities and Coulombic efficiencies plotted against cycle numbers under freestanding condition (E), alternating freestanding/10% stretching condition (F), and alternating freestanding/folding condition (G).

reduction could be due to a slight increase in the area of active material being deformed during folding (Figure S10).

Moreover, we tested the stability of the holey battery against deformation cycles. The holey battery underwent an initial cycle

free of deformation (Figure S11A), followed by 100 stretch/free cycles with subsequent cycling (Figure S11B). Then, it experienced 100 bending/free cycles and underwent cycling once again (Figure S11C). All three charge-discharge profiles exhibit

good similarities, affirming the holey battery's ability to endure multiple deformation cycles. We also tested the performance of the battery under a 45° twisting condition, in which over 85% capacity retention was obtained compared to its free-standing state (Figure S12). Additionally, the battery remained functional even after washing (Figure S13). To showcase the enhancement of the capacity of the holey batteries, we fabricated and cycled a double-layer holey battery without applying deformation. The cycling performance of the double-layer battery remains stable, as depicted in Figure S14, achieving an areal capacity of 14.4 mW h/cm². Additional layers could potentially yield a higher areal energy density while maintaining favorable mechanical properties, but this would depend on achieving high sample consistency and precise alignment. The heat generated during discharge can pose challenges for wearable applications.⁶¹ However, in our application, the holey battery can be charged off the body, so heating during charging is not a concern. During discharge, with the total power consumption at the mW level, heat generation will be below the mW level—minimal enough to dissipate easily through airflow.⁶² Therefore, heat generation is unlikely to pose an issue for this particular application.

In conclusion, the holey battery demonstrates the ability to undergo 10% stretching and 180° folding with minimal impact on its electrochemical performance, thereby establishing its suitability for wearable battery applications.

Conclusion

In summary, we have developed a holey battery design guided by the FEM that enhances the stretchability and breathability of pouch cells without compromising their areal energy density. The hole structure in the battery does not adversely affect its electrochemical performance. A capacity of 149 mA h/g and a retention of 95% after 100 cycles can be obtained at a current density of 75 mA/g, with a mass loading of LFP up to 15 mg/cm². Furthermore, through the strategic design of hole patterns, guided by FEM analysis, we found a hole pattern leading to a small percentage of largely strained areas. The electrochemical performance of the holey battery is maintained when subjected to either 10% diagonal stretching (>90% capacity) or 180° folding (>95% capacity), with the capacity being recoverable upon the release of external deformation forces. The areal energy density achieved is 7.2 mW h/cm² in a single-layer pouch, which is scalable to 14.4 mW h/cm² using double electrode layers. Moreover, the breathability of these batteries was found to be twice that of cotton cloth, indicating that their integration into clothing will not diminish the wearer's comfort. In addition to its outstanding stretchability and breathability, the design of the holey battery does not necessitate the use of novel chemicals, inactive additives, or unique fabrication processes. It is fully compatible with commercially available electrode materials and consumables. The hot-pressing technique employed in its construction is also compatible with current pouch cell fabrication facilities, and the additional process of making holes can be effectively scaled up using laser cutting or blade cutting techniques. It is important to note that more precise cutting and alignment techniques are essential for large-scale manufacturing of the holey battery. Without these, local stress concentrations

around the hole corners could result in tearing and air leakage, while misalignment could lead to short circuits. Both types of failures increase the risk of fire hazards in the device. Therefore, the safety tolerances are highly dependent on manufacturing precision and defect minimization.

In conclusion, the development of the holey battery represents a promising and scalable method for fabricating comfortable, wearable batteries for wearable electronics using commercially available materials and equipment, significantly reducing the complexity associated with the production of such devices.

METHODS

Finite element modeling

The commercial finite element code ABAQUS/Explicit 2022 was used in the present study. The precision of the modeling results is ensured by a global mesh size of 0.5 mm in the element type of C3D8R (8-node linear brick, reduced integration, hourglass control). All modeled battery pouches have a side length of 10 cm, while the total areas of the holes are kept the same for pouches with different shapes. Linear elastic material properties with a density of 2.7 g/cm³, a Young's modulus of 70 GPa, and a Poisson's ratio of 0.33 were adopted for the battery pouch. A Python package was developed to count the number of elements in the models with a maximum principal strain greater than the applied stretch in order to estimate the failed area of the simulated battery panels under a variety of large deformations.

Materials

LFP powder (MTI) was used as the cathode active material, and graphite powder (MTI) was used as the anode active material. Ketjenblack powder (<50 nm, MSE Supplies) was used as a conductive additive. A Celgard 2500 membrane was used as the separator. Polyvinylidene fluoride (PVDF) powder (MTI) served as the binder, and N-methyl-2-pyrrolidone (NMP; 99.5%, Sigma-Aldrich) acted as the solvent. Aluminum foil, copper foil, and laminated aluminum were purchased from MTI. 1.0 M lithium hexafluorophosphate (LiPF₆) solution, in 50/50 (v/v) ethylene carbonate (EC) and dimethyl carbonate (DMC) (battery grade, Sigma-Aldrich), was used as the electrolyte. Silica gel (230–400 mesh, Natland International) was used as the desiccant for the breathability test.

Fabrication of electrodes

Electrodes were prepared using a conventional slurry method. Electrode particles, carbon black, and a PVDF binder with a mass ratio of 90:5:5 were dispersed in NMP. After stirring overnight, the cathode slurry was cast onto a carbon-coated Al foil, and the anode slurry was cast onto a Cu foil, both with a doctor blade, and dried at 120°C in a vacuum oven for 12 h. The mass loading of the cathode was about 15 mg/cm², and the mass loading of the anode was about 7 mg/cm².

Assembling and sealing the battery

Precise holes were cut into the laminated aluminum foil, active material-coated foils, and the Celgard separator using razor blades. Then, the separator layer was sandwiched between the anode and cathode foils, with two sheets of laminated

aluminum foil on the top and bottom. Then, the holes were sealed using a compact vacuum sealer (Model MSK-115A-S, MTI) with attached bars made of stainless steel within a glovebox. Subsequently, three edges of the cell were sealed to prevent any electrolyte leakage, and 1 M lithium hexafluorophosphate in a 1:1 (v/v) EC/DMC electrolyte was injected into the cell. Finally, the fourth side of the cell was sealed under vacuum.

Breathability test

The breathability of the battery was evaluated using a constant temperature and humidity chamber (model LHS-150HC-11) under controlled environmental conditions of 25°C and 70% humidity. To conduct the experiment, the holey battery was double-sided taped to the top of a container having 60 g of silica gel, while other containers with the same amount of silica gel were used as controls with cotton cloth and laminated aluminum with no holes. The masses of all containers were measured every 24 h for 11 days.

Battery test

A defined cycling profile was performed using a Bio-logic VMP-3e potentiostat, including charging and discharging phases for a voltage range from 2.6 to 4 V at a constant current density of 75 mA/g LFP. The cycling profile was tested under conditions including no deformation, with 10% diagonal stretching, and with 180° bending. All deformation was applied using an Instron 3367 tensile testing machine. The battery was also woven onto a lab coat using cotton yarn to demonstrate its functionality.

RESOURCE AVAILABILITY

Lead contact

Requests for further information and resources should be directed to and will be fulfilled by the lead contact, Liangbing Hu (liangbing.hu@yale.edu).

Materials availability

This study did not generate new unique reagents.

Data and code availability

All data reported in this paper will be shared by the lead contact upon request.

ACKNOWLEDGMENTS

The project is not directly funded. We acknowledge the support from the University of Maryland A. James Clark School of Engineering, the University of Maryland supercomputing resources (<https://hpcc.umd.edu>), and the Maryland Advanced Research Computing Center (MARCC) for conducting the research reported in this work.

AUTHOR CONTRIBUTIONS

L.H., Teng Li, and L.X. designed the experiments. L.X., S.V.P., E.P., and C.W. carried out the fabrication of the holey batteries. Q.C. and L.W. conducted FEM modeling. L.X., Tanguan Li, X.Z., C.Y., and K.J. conducted the electrochemical and physical characterization. L.H., Teng Li, L.X., Q.C., S.V.P., and P.L. collectively wrote the paper. All authors commented on the final manuscript.

DECLARATION OF INTERESTS

We, the authors, have a patent application: US provisional application no. 63/374,673. Title: Devices, Systems, and Methods for Breathable Wearable Bat-

teries via Hole-Array Structures. Filing date: September 6, 2022. Inventors: L.H., L.X., and P.L.

SUPPLEMENTAL INFORMATION

Supplemental information can be found online at <https://doi.org/10.1016/j.matt.2025.101959>.

Received: July 13, 2024

Revised: November 19, 2024

Accepted: January 2, 2025

Published: January 24, 2025

REFERENCES

1. Wang, X., Lu, X., Liu, B., Chen, D., Tong, Y., and Shen, G. (2014). Flexible Energy-Storage Devices: Design Consideration and Recent Progress. *Adv. Mater.* 26, 4763–4782. <https://doi.org/10.1002/adma.201400910>.
2. Pu, X., Li, L., Song, H., Du, C., Zhao, Z., Jiang, C., Cao, G., Hu, W., and Wang, Z.L. (2015). A Self-Charging Power Unit by Integration of a Textile Triboelectric Nanogenerator and a Flexible Lithium-Ion Battery for Wearable Electronics. *Adv. Mater.* 27, 2472–2478. <https://doi.org/10.1002/adma.201500311>.
3. Hsu, P.-C., Song, A.Y., Catrysse, P.B., Liu, C., Peng, Y., Xie, J., Fan, S., and Cui, Y. (2016). Radiative human body cooling by nanoporous polyethylene textile. *Science* 353, 1019–1023. <https://doi.org/10.1126/science.aaf5471>.
4. Li, C., Cao, R., and Zhang, X. (2018). Breathable Materials for Triboelectric Effect-Based Wearable Electronics. *Appl. Sci.* 8, 2485. <https://doi.org/10.3390/app8122485>.
5. Wang, D., Han, C., Mo, F., Yang, Q., Zhao, Y., Li, Q., Liang, G., Dong, B., and Zhi, C. (2020). Energy density issues of flexible energy storage devices. *Energy Storage Mater.* 28, 264–292. <https://doi.org/10.1016/j.ensm.2020.03.006>.
6. Mo, F., Liang, G., Huang, Z., Li, H., Wang, D., and Zhi, C. (2020). An Overview of Fiber-Shaped Batteries with a Focus on Multifunctionality, Scalability, and Technical Difficulties. *Adv. Mater.* 32, e1902151. <https://doi.org/10.1002/adma.201902151>.
7. Zhou, Y., Wang, C.H., Lu, W., and Dai, L. (2020). Recent Advances in Fiber-Shaped Supercapacitors and Lithium-Ion Batteries. *Adv. Mater.* 32, e1902779. <https://doi.org/10.1002/adma.201902779>.
8. Ge, X., Zhang, W., Song, F., Xie, B., Li, J., Wang, J., Wang, X., Zhao, J., and Cui, G. (2022). Single-Ion-Functionalized Nanocellulose Membranes Enable Lean-Electrolyte and Deeply Cycled Aqueous Zinc-Metal Batteries. *Adv. Funct. Mater.* 32, 1–11. <https://doi.org/10.1002/adfm.202200429>.
9. Shi, H.H., Pan, Y., Xu, L., Feng, X., Wang, W., Potluri, P., Hu, L., Hasan, T., and Huang, Y.Y.S. (2023). Sustainable electronic textiles towards scalable commercialization. *Nat. Mater.* 22, 1294–1303. <https://doi.org/10.1038/s41563-023-01615-z>.
10. Li, H., Tang, Z., Liu, Z., and Zhi, C. (2019). Evaluating Flexibility and Wearability of Flexible Energy Storage Devices. *Joule* 3, 613–619. <https://doi.org/10.1016/j.joule.2019.01.013>.
11. Zeng, L., Qiu, L., and Cheng, H.-M. (2019). Towards the practical use of flexible lithium ion batteries. *Energy Storage Mater.* 23, 434–438. <https://doi.org/10.1016/j.ensm.2019.04.019>.
12. Wu, Z., Wang, Y., Liu, X., Lv, C., Li, Y., Wei, D., and Liu, Z. (2019). Carbon-Nanomaterial-Based Flexible Batteries for Wearable Electronics. *Adv. Mater.* 31, e1800716. <https://doi.org/10.1002/adma.201800716>.
13. Yang, Q., Chen, A., Li, C., Zou, G., Li, H., and Zhi, C. (2021). Categorizing wearable batteries: Unidirectional and omnidirectional deformable batteries. *Matter* 4, 3146–3160. <https://doi.org/10.1016/j.matt.2021.07.016>.
14. Liu, Y., Lin, D., Yuen, P.Y., Liu, K., Xie, J., Dauskardt, R.H., and Cui, Y. (2017). An Artificial Solid Electrolyte Interphase with High Li-Ion Conductivity,

- Mechanical Strength, and Flexibility for Stable Lithium Metal Anodes. *Adv. Mater.* 29, 1605531. <https://doi.org/10.1002/adma.201605531>.
15. Yue, X., Liu, H., and Liu, P. (2019). Polymer grafted on carbon nanotubes as a flexible cathode for aqueous zinc ion batteries. *Chem. Commun.* 55, 1647–1650. <https://doi.org/10.1039/C8CC10060H>.
 16. Li, Y., Wang, D., An, Q., Ren, B., Rong, Y., and Yao, Y. (2016). Flexible electrode for long-life rechargeable sodium-ion batteries: effect of oxygen vacancy in MoO₃-x. *J. Mater. Chem. A* 4, 5402–5405. <https://doi.org/10.1039/C6TA01342B>.
 17. Tao, L., Xu, Z., Kuai, C., Zheng, X., Wall, C.E., Jiang, C., Esker, A.R., Zheng, Z., and Lin, F. (2020). Flexible lignin carbon membranes with surface ozonolysis to host lean lithium metal anodes for nickel-rich layered oxide batteries. *Energy Storage Mater.* 24, 129–137. <https://doi.org/10.1016/j.ensm.2019.08.027>.
 18. Ashok Kumar, A., Thirumurugan, V., Gopalakrishnan, M., and Priyalatha, S. (2021). Analysis of Deformation for Active Sports Wears. *Latest Trends Text. Fash. Des.* 3, 676–687. <https://doi.org/10.32474/LTTFD.2021.03.000175>.
 19. Ghadi, B.M., Hekmatnia, B., Fu, Q., and Ardebili, H. (2023). Stretchable fabric-based lithium-ion battery. *Extreme Mech. Lett.* 67, 102026. <https://doi.org/10.1016/j.eml.2023.102026>.
 20. Zhou, G., Lin, X., Liu, J., Yu, J., Wu, J., Law, H.M., Wang, Z., and Ciucci, F. (2021). In situ formation of poly(butyl acrylate)-based non-flammable elastic quasi-solid electrolyte for dendrite-free flexible lithium metal batteries with long cycle life for wearable devices. *Energy Storage Mater.* 34, 629–639. <https://doi.org/10.1016/j.ensm.2020.10.012>.
 21. Karami-Mosammam, M., Danninger, D., Schiller, D., and Kaltenbrunner, M. (2022). Stretchable and Biodegradable Batteries with High Energy and Power Density. *Adv. Mater.* 34, 2204457. <https://doi.org/10.1002/adma.202204457>.
 22. Hong, S., Lee, J., Do, K., Lee, M., Kim, J.H., Lee, S., and Kim, D. (2017). Stretchable Electrode Based on Laterally Combed Carbon Nanotubes for Wearable Energy Harvesting and Storage Devices. *Adv. Funct. Mater.* 27, 1704353. <https://doi.org/10.1002/adfm.201704353>.
 23. Zhang, Y., Zhao, Y., Ren, J., Weng, W., and Peng, H. (2016). Advances in Wearable Fiber-Shaped Lithium-Ion Batteries. *Adv. Mater.* 28, 4524–4531. <https://doi.org/10.1002/adma.201503891>.
 24. Song, W., Yoo, S., Song, G., Lee, S., Kong, M., Rim, J., Jeong, U., and Park, S. (2019). Recent Progress in Stretchable Batteries for Wearable Electronics. *Batter. Supercaps* 2, 181–199. <https://doi.org/10.1002/batt.201800140>.
 25. Wen, J., Xu, B., Gao, Y., Li, M., and Fu, H. (2021). Wearable technologies enable high-performance textile supercapacitors with flexible, breathable and wearable characteristics for future energy storage. *Energy Storage Mater.* 37, 94–122. <https://doi.org/10.1016/j.ensm.2021.02.002>.
 26. Zeng, Y., Zhang, X., Meng, Y., Yu, M., Yi, J., Wu, Y., Lu, X., and Tong, Y. (2017). Achieving Ultrahigh Energy Density and Long Durability in a Flexible Rechargeable Quasi-Solid-State Zn–MnO₂ Battery. *Adv. Mater.* 29, 1700274. <https://doi.org/10.1002/adma.201700274>.
 27. Liu, Z., Li, H., Zhu, M., Huang, Y., Tang, Z., Pei, Z., Wang, Z., Shi, Z., Liu, J., Huang, Y., et al. (2018). Towards wearable electronic devices: A quasi-solid-state aqueous lithium-ion battery with outstanding stability, flexibility, safety and breathability. *Nano Energy* 44, 164–173. <https://doi.org/10.1016/j.nanoen.2017.12.006>.
 28. Liu, Z., Yang, Q., Wang, D., Liang, G., Zhu, Y., Mo, F., Huang, Z., Li, X., Ma, L., Tang, T., et al. (2019). A Flexible Solid-State Aqueous Zinc Hybrid Battery with Flat and High-Voltage Discharge Plateau. *Adv. Energy Mater.* 9, 1902473. <https://doi.org/10.1002/aenm.201902473>.
 29. Ouyang, G., Whang, G., MacInnis, E., and Iyer, S.S. (2021). Fabrication of Flexible Ionic-Liquid Thin Film Battery Matrix on FlexTrate™ for Powering Wearable Devices. In 2021 IEEE 71st Electronic Components and Technology Conference (ECTC) (IEEC), pp. 1620–1626. <https://doi.org/10.1109/ECTC32696.2021.00257>.
 30. Yang, C., Ji, X., Fan, X., Gao, T., Suo, L., Wang, F., Sun, W., Chen, J., Chen, L., Han, F., et al. (2017). Flexible Aqueous Li-Ion Battery with High Energy and Power Densities. *Adv. Mater.* 29, 1701972. <https://doi.org/10.1002/adma.201701972>.
 31. Weng, G.-M., Simon Tam, L.-Y., and Lu, Y.-C. (2017). High-performance LiTi₂(PO₄)₃ anodes for high-areal-capacity flexible aqueous lithium-ion batteries. *J. Mater. Chem. A* 5, 11764–11771. <https://doi.org/10.1039/C7TA00482F>.
 32. Huang, Y., Fang, C., Zeng, R., Liu, Y., Zhang, W., Wang, Y., Liu, Q., and Huang, Y. (2017). In Situ-Formed Hierarchical Metal–Organic Flexible Cathode for High-Energy Sodium-Ion Batteries. *ChemSusChem* 10, 4704–4708. <https://doi.org/10.1002/cssc.201701484>.
 33. Meng, Q., Wu, H., Mao, L., Yuan, H., Ahmad, A., and Wei, Z. (2017). Combining Electrode Flexibility and Wave-Like Device Architecture for Highly Flexible Li-Ion Batteries. *Adv. Mater. Technol.* 2, 1700032. <https://doi.org/10.1002/admt.201700032>.
 34. Kumar, R., Shin, J., Yin, L., You, J., Meng, Y.S., and Wang, J. (2017). All-Printed, Stretchable Zn–Ag₂O Rechargeable Battery via Hyperelastic Binder for Self-Powering Wearable Electronics. *Adv. Energy Mater.* 7, 1602096. <https://doi.org/10.1002/aenm.201602096>.
 35. Wang, Z., Li, X., Yang, Z., Guo, H., Tan, Y.J., Susanto, G.J., Cheng, W., Yang, W., and Tee, B.C.K. (2021). Fully transient stretchable fruit-based battery as safe and environmentally friendly power source for wearable electronics. *EcoMat* 3, e12073. <https://doi.org/10.1002/eom2.12073>.
 36. Bai, C., Ji, K., Feng, S., Zhang, J., and Kong, D. (2022). An intrinsically stretchable aqueous Zn–MnO₂ battery based on microcracked electrodes for self-powering wearable electronics. *Energy Storage Mater.* 47, 386–393. <https://doi.org/10.1016/j.ensm.2022.02.032>.
 37. Yu, X., Ma, S., Zhang, Q., Hou, Y., He, Q., Luo, Y., and Gao, X. (2023). Stretchable high-capacity SiO_x/carbon anode with good cycle stability enabled by a triblock copolymer elastomer. *Eur. Polym. J.* 190, 111989. <https://doi.org/10.1016/j.eurpolymj.2023.111989>.
 38. Huang, X., Liu, Y., Park, W., Zhao, Z., Li, J., Lim, C.K., Wong, T.H., Yiu, C.K., Gao, Y., Zhou, J., et al. (2023). Stretchable magnesium–air battery based on dual ions conducting hydrogel for intelligent biomedical applications. *InfoMat* 5, e12388. <https://doi.org/10.1002/inf2.12388>.
 39. Shen, Q., Jiang, M., Wang, R., Song, K., Vong, M.H., Jung, W., Krisnadi, F., Kan, R., Zheng, F., Fu, B., et al. (2023). Liquid metal-based soft, hermetic, and wireless-communicable seals for stretchable systems. *Science* 379, 488–493. <https://doi.org/10.1126/science.ade7341>.
 40. Zhang, Y., Wang, L., Guo, Z., Xu, Y., Wang, Y., and Peng, H. (2016). High-Performance Lithium–Air Battery with a Coaxial-Fiber Architecture. *Angew. Chemie* 128, 4563–4567. <https://doi.org/10.1002/ange.201511832>.
 41. Li, Q., Zhang, Q., Liu, C., Sun, J., Guo, J., Zhang, J., Zhou, Z., He, B., Pan, Z., and Yao, Y. (2019). Flexible all-solid-state fiber-shaped Ni–Fe batteries with high electrochemical performance. *J. Mater. Chem. A* 7, 520–530. <https://doi.org/10.1039/C8TA09822K>.
 42. He, J., Lu, C., Jiang, H., Han, F., Shi, X., Wu, J., Wang, L., Chen, T., Wang, J., Zhang, Y., et al. (2021). Scalable production of high-performing woven lithium-ion fibre batteries. *Nature* 597, 57–63. <https://doi.org/10.1038/s41586-021-03772-0>.
 43. Chen, A., Guo, X., Yang, S., Liang, G., Li, Q., Chen, Z., Huang, Z., Yang, Q., Han, C., and Zhi, C. (2021). Human joint-inspired structural design for a bendable/foldable/stretchable/twistable battery: achieving multiple deformabilities. *Energy Environ. Sci.* 14, 3599–3608. <https://doi.org/10.1039/D1EE00480H>.
 44. Praveen, S., Kim, T., Jung, S.P., and Lee, C.W. (2023). 3D-Printed Silicone Substrates as Highly Deformable Electrodes for Stretchable Li-Ion Batteries. *Small* 19, e2205817. <https://doi.org/10.1002/smll.202205817>.
 45. Xiao, X., Xiao, X., Zhou, Y., Zhao, X., Chen, G., Liu, Z., Wang, Z., Lu, C., Hu, M., Nashalian, A., et al. (2021). An ultrathin rechargeable solid-state zinc ion fiber battery for electronic textiles. *Sci. Adv.* 7, eabl3742. <https://doi.org/10.1126/sciadv.abl3742>.

46. Kwon, Y.H., Woo, S.W., Jung, H.R., Yu, H.K., Kim, K., Oh, B.H., Ahn, S., Lee, S.Y., Song, S.W., Cho, J., et al. (2012). Cable-Type Flexible Lithium Ion Battery Based on Hollow Multi-Helix Electrodes. *Adv. Mater.* *24*, 5192–7–5145. <https://doi.org/10.1002/adma.201202196>.
47. Peng, L., Fang, Z., Zhu, Y., Yan, C., and Yu, G. (2018). Holey 2D Nanomaterials for Electrochemical Energy Storage. *Adv. Energy Mater.* *8*, 1702179. <https://doi.org/10.1002/aenm.201702179>.
48. Peng, L., Xiong, P., Ma, L., Yuan, Y., Zhu, Y., Chen, D., Luo, X., Lu, J., Amine, K., and Yu, G. (2017). Holey two-dimensional transition metal oxide nanosheets for efficient energy storage. *Nat. Commun.* *8*, 15139. <https://doi.org/10.1038/ncomms15139>.
49. Sun, H., Zhu, J., Baumann, D., Peng, L., Xu, Y., Shakir, I., Huang, Y., and Duan, X. (2018). Hierarchical 3D electrodes for electrochemical energy storage. *Nat. Rev. Mater.* *4*, 45–60. <https://doi.org/10.1038/s41578-018-0069-9>.
50. Yu, K.J., Yan, Z., Han, M., and Rogers, J.A. (2017). Inorganic semiconducting materials for flexible and stretchable electronics. *npj Flex. Electron.* *1*, 4. <https://doi.org/10.1038/s41528-017-0003-z>.
51. He, J., Nuzzo, R.G., and Rogers, J.A. (2015). Inorganic Materials and Assembly Techniques for Flexible and Stretchable Electronics. *Proc. IEEE* *103*, 619–632. <https://doi.org/10.1109/JPROC.2015.2396991>.
52. Khan, Y., Ostfeld, A.E., Lochner, C.M., Pierre, A., and Arias, A.C. (2016). Monitoring of Vital Signs with Flexible and Wearable Medical Devices. *Adv. Mater.* *28*, 4373–4395. <https://doi.org/10.1002/adma.201504366>.
53. Manjakkal, L., Yin, L., Nathan, A., Wang, J., and Dahiya, R. (2021). Energy Autonomous Sweat-Based Wearable Systems. *Adv. Mater.* *33*, e2100899. <https://doi.org/10.1002/adma.202100899>.
54. Baranov, A., Spirjakin, D., Akbari, S., and Somov, A. (2015). Optimization of power consumption for gas sensor nodes: A survey. *Sensor. Actuator. A Phys.* *233*, 279–289. <https://doi.org/10.1016/j.sna.2015.07.016>.
55. Timoshenko, S.P., and Goodier, J.N. (1969). *Theory of Elasticity (McGraw-Hill)*.
56. Tucker, M.B., and Li, T. (2009). Strain deconcentration in thin films patterned with circular holes. *Int. J. Appl. Mech.* *01*, 557–568. <https://doi.org/10.1142/S1758825109000307>.
57. Dong, L., Fan, K., Feng, Y., Zhao, M., Qin, X., Zhu, Z., and Li, C. (2022). Preparation Technology of Stretchable Electrode Based on Laser Cutting. *Machines* *10*, 854. <https://doi.org/10.3390/machines10100854>.
58. Xu, R., He, P., Lan, G., Behrouzi, K., Peng, Y., Wang, D., Jiang, T., Lee, A., Long, Y., and Lin, L. (2022). Facile Fabrication of Multilayer Stretchable Electronics via a Two-mode Mechanical Cutting Process. *ACS Nano* *16*, 1533–1546. <https://doi.org/10.1021/acsnano.1c10011>.
59. Jansson, E., Korhonen, A., Hietala, M., and Kololuoma, T. (2020). Development of a full roll-to-roll manufacturing process of through-substrate vias with stretchable substrates enabling double-sided wearable electronics. *Int. J. Adv. Manuf. Technol.* *111*, 3017–3027. <https://doi.org/10.1007/s00170-020-06324-4>.
60. Mustapha, R., Zoughaib, A., Ghaddar, N., and Ghali, K. (2020). Modified up-right cup method for testing water vapor permeability in porous membranes. *Energy* *195*, 117057. <https://doi.org/10.1016/j.energy.2020.117057>.
61. Muralee Gopi, C.V., Vinodh, R., Sambasivam, S., Obaidat, I.M., and Kim, H.-J. (2020). Recent progress of advanced energy storage materials for flexible and wearable supercapacitor: From design and development to applications. *J. Energy Storage* *27*, 101035. <https://doi.org/10.1016/j.est.2019.101035>.
62. Sun, Y., Li, Y.-Z., and Yuan, M. (2023). Requirements, challenges, and novel ideas for wearables on power supply and energy harvesting. *Nano Energy* *115*, 108715. <https://doi.org/10.1016/j.nanoen.2023.108715>.